12th IMEKO TC10 Workshop on Technical Diagnostics
New Perspectives in Measurements, Tools and Techniques for Industrial Applications
June 6-7, 2013, Florence, Italy

Stator Winding Fault Diagnosis in Permanent Magnet Synchronous Generators Based on Short-Circuited Turns Identification Using Extended Kalman Filter.

B. Aubert [1,2,3], J. Regnier [1,2], S. Caux [1,2], D. Alejo [3]

[1] *Université de Toulouse ; INPT, UPS ; LAPLACE (Laboratoire Plasma et Conversion d'Energie) ; ENSEEIHT, 2 rue Charles Camichel, BP 7122, F-31071 Toulouse cedex 7, France*
[2] *CNRS ; LAPLACE ; F-31071 Toulouse, France*
[3] *AEROCONSEIL – AKKA TECHNOLOGIES GROUP ; 3 rue Dieudonné Costes; F-31703 Blagnac, France.*

Abstract- This paper deals with an Extended Kalman Filter (EKF) based fault detection for inter-turn short-circuit in Permanent Magnet Synchronous Generators (PMSG). A specific faulty model in d-q frame is developed to estimate the number of short-circuited turns which are used to a fault indicator setting up. Simulation results demonstrate the sensitivity and the robustness of the chosen indicator against various operation points on an electrical network.

I. Introduction

Permanent Magnet Synchronous Generators (PMSG) are increasingly used in various industrial fields such as aerospace, railway and automotive sectors or renewable energy [1]-[2] to take advantage of its high efficiency, small size and easy control for variable-speed applications compared to a wounded rotor design. With regard to safety considerations, the main drawback of PMSG is the critical effect of inter-turn short-circuits in stator windings, which are the root of highest fault current [3], through permanent rotor flux which allows stator short-circuit current flowing as long as the machine is rotating. Thus, an early on-line detection is required to perform the appropriate safety request and to avoid greater deterioration. As well as being prompt, the detection method should be robust to external constraints (as power or speed variation) to avoid false alarms. Moreover, the constraints related to on-line monitoring considerations imply a detection algorithm matching the performances of on-board computers.
To match these requirements, this paper proposes an identification of the number of short-circuited turns based on a faulty PMSG model in Park frame using an Extended Kalman Filter (EKF) algorithm. This paper is organized as follow: in section II, the faulty PMSG Park model used for fault diagnosis is described. Section III presents simulation results of the EKF algorithms in both healthy and faulty conditions. The proposed fault indicator build is also described. Finally, a robustness and a sensitivity study are presented in section IV to assess the proposed indicator effectiveness.

II. Faulty PMSG model for inter-turn short-circuit detection

The faulty PMSG model used for inter-turn short-circuit detection is based on a former study [4] with less modelling assumptions (voltage drops due to short-circuit reduction is taken into account) to make the PMSG model more sensitive to windings faults. The model enables the fault localization with the use of angle $\theta_{s/c}$ (equal to 0, $2\pi/3$ or $4\pi/3$ for a short-circuit respectively on phase A, phase B or phase C) and the number of short-circuit turns $n_{s/c}$ (ratio between short-circuited turns and the whole turns on a stator winding). Figure 1 shows the basic model for fault diagnosis with inter-turn short-circuit on phase C ($\theta_{s/c} = 4\pi/3$).

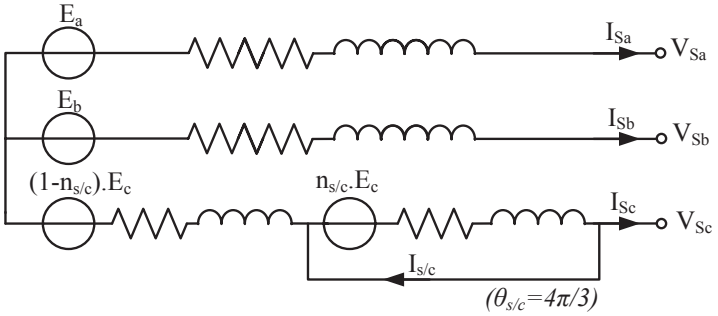

Figure 1. Inter-turn short-circuit model used for fault diagnosis

According to this faulty model, the stator voltages and the short-circuit loop equations are given in (1):

$$\begin{cases} [V_S] = -R_S.[I_S] - [L].[\dot{I}_S] + [E] - n_{s/c}.R_S.T_{s/c}.I_{s/c} - \sqrt{\frac{3}{2}}.n_{s/c}.L_{ps}.T_{32}.\begin{bmatrix}\cos\theta_{s/c}\\ \sin\theta_{s/c}\end{bmatrix}.\dot{I}_{s/c} - n_{s/c}.L_{ls}.T_{s/c}.\dot{I}_{s/c} \\ 0 = n_{s/c}.R_S.T_{s/c}{}^T.[I_S] + \sqrt{\frac{3}{2}}.n_{s/c}.L_{ps}.\left(T_{32}.\begin{bmatrix}\cos\theta_{s/c}\\ \sin\theta_{s/c}\end{bmatrix}\right)^T.[\dot{I}_S] - n_{s/c}.T_{s/c}{}^T.[E] + n_{s/c}.R_S.I_{s/c} \\ \quad + n_{s/c}{}^2.(L_{ms}+L_{ls}).\dot{I}_{s/c} + n_{s/c}.L_{ls}.T_{s/c}{}^T.[\dot{I}_S] \end{cases} \quad (1)$$

Where:

$[V_S]=[V_{Sa}V_{Sb}V_{Sc}]$: Stator voltages vector
$[I_s]=[I_{sa}I_{sb}I_{sc}]$: Stator currents vector
$I_{s/c}$: Short-circuit current
$[E_s]=[E_aE_bE_c]$: Electromotive forces vector
R_S : Stator resistance
$[L]=\begin{bmatrix}L_{ls}+L_{ps} & -L_{ps}/2 & -L_{ps}/2\\ -L_{ps}/2 & L_{ls}+L_{ps} & -L_{ps}/2\\ -L_{ps}/2 & -L_{ps}/2 & L_{ls}+L_{ps}\end{bmatrix}$: Stator inductances matrix
$[T_{32}]=\frac{1}{\sqrt{3}}\begin{bmatrix}\sqrt{2} & 0\\ -1/\sqrt{2} & \sqrt{3/2}\\ -1/\sqrt{2} & -\sqrt{3/2}\end{bmatrix}$: Concordia transformation matrix
$T_{s/c}=\frac{1}{3}.\begin{bmatrix}1+2.\cos(\theta_{s/c})\\ 1+2.\cos\left(\theta_{s/c}-\frac{2\pi}{3}\right)\\ 1+2.\cos\left(\theta_{s/c}-\frac{4\pi}{3}\right)\end{bmatrix}$: Short-circuit matrix $\left(=\begin{bmatrix}1\\0\\0\end{bmatrix}\text{ if }\theta_{s/c}=0;=\begin{bmatrix}0\\1\\0\end{bmatrix}\text{ if }\theta_{s/c}=\frac{2\pi}{3};=\begin{bmatrix}0\\0\\1\end{bmatrix}\text{ if }\theta_{s/c}=\frac{4\pi}{3}\right)$

With Park transformation applied to (1) and some change of variables on $I_{s/c}$ and I_s, the faulty model can be expressed as follow:

$$\begin{cases} [V_S]_{dq} = -R_S.[I'_S]_{dq} - \omega.L_S.\begin{bmatrix}0 & -1\\ 1 & 0\end{bmatrix}.[I'_S]_{dq} - L_S.[\dot{I}'_S]_{dq} + [E]_{dq} \\ [I_S]_{dq} = [I'_S]_{dq} - [\tilde{I}_{s/c}]_{dq} = [I'_S]_{dq} - \frac{1}{[Z_{s/c}]_{dq}}.[V_S]_{dq} \end{cases} \quad (2)$$

Where:

$L_S = 3/2.L_{ps} + L_{ls}$: Stator synchronous inductance
$\frac{1}{[Z_{s/c}]_{dq}} = \frac{2.n_{s/c}}{(3-2.n_{s/c}).R_S}.P(\theta)^T.Q(\theta_{s/c}).P(\theta)$: Equivalent short-circuit fault impedance
$P(\theta) = \begin{bmatrix}\cos\theta & -\sin\theta\\ \sin\theta & \cos\theta\end{bmatrix}$: Park transformation matrix
$Q(\theta_{s/c}) = \begin{bmatrix}\cos^2(\theta_{s/c}) & \cos(\theta_{s/c}).\sin(\theta_{s/c})\\ \cos(\theta_{s/c}).\sin(\theta_{s/c}) & \sin^2(\theta_{s/c})\end{bmatrix}$: Fault localization matrix
$[\tilde{I}_{s/c}]_{dq} = P(\theta)^T.\sqrt{\frac{2}{3}}.n_{s/c}.\begin{bmatrix}\cos(\theta_{s/c})\\ \sin(\theta_{s/c})\end{bmatrix}.I_{s/c}$: Short-circuit current calculation in dq frame
$[I'_S]_{dq} = [I_S]_{dq} + [\tilde{I}_{s/c}]_{dq}$: Stator current calculation in dq frame

It can be noticed that (2) is the same equation as a classical PMSG taking account $[I_S']$ as the stator current with the addition of a faulty equation. The short-circuit current is represented by the equivalent fault impedance $[Z_{s/c}]$ at the output of the machine which deflects a part of the stator current. Expending this model to each phase, three short-circuit impedances ($Z_{s/c1}$, $Z_{s/c2}$, $Z_{s/c3}$ for $\theta_{s/c}=0$, $2\pi/3$, $4\pi/3$ respectively) are added to the PMSG model as shown on Figure 2.

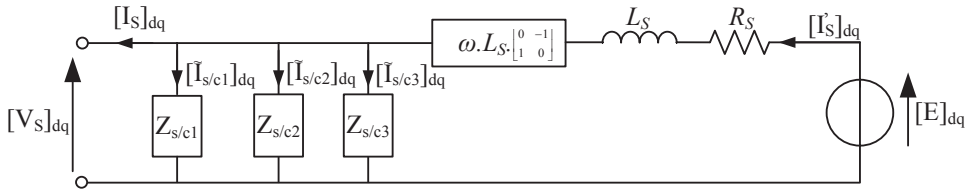

Figure 2. Global inter-turn faulty PMSG model in Park's frame

This model can be written as a state space representation with $[I_S']$ as the state vector. The inter-turn fault is expressed in the feedforward matrix D, depending on the number of short-circuited turns $n_{s/c1}$, $n_{s/c2}$, $n_{s/c3}$.
To estimate these parameters in this non-linear model, the EKF algorithm is used. In EKF algorithm, a special attention should be paid to covariance matrices tuning, particularly for the measurement noises covariance matrix R and the state noises covariance matrix Q to let the estimated parameter dynamic response high and also take into account model variations [5]. In order to satisfy the fast dynamic response requirement for the fault indicator, the covariance matrices used for the estimation of $\left(\hat{n}_{s/c}\right)_i$ are expressed in (3):

$$\begin{cases} P_0 = 10^{-1}.I_{5\times5};\ R = 10^{-2}.I_{2\times2} \\ Q = 10^{-5}.\begin{bmatrix} I_{2\times2} & 0 \\ 0 & 10^{-4}.I_{3\times3} \end{bmatrix} \end{cases} \quad (3)$$

Simulations results are presented in the following section.

III. Simulation Procedure

A. Simulation Test Bench Setup

The faulty PMSG model used for simulation is based on Electrically Coupled Magnetic Circuit (ECMC) [6]. It consists in a semi-analytical computation of the PMSG inductances from the stator winding layout including additional connections for inter-turn short-circuit generation. Thus, several faulty PMSG models have been created with 4%, 8%, 12% and 16% of short-circuit turns in the stator winding, respectively corresponding to 3, 6, 9 and 12 turns on 72 whole turns of a stator winding. The simulation test bench is set with SABER software in order to generate various operating points for the faulty PMSG model (Figure 3). It is composed by a balanced R-L load to vary the electrical power and the power factor, an unbalanced R load to create power unbalanced and a harmonic load including a three-phase diode bridge rectifier with resistive load to generate current harmonics.

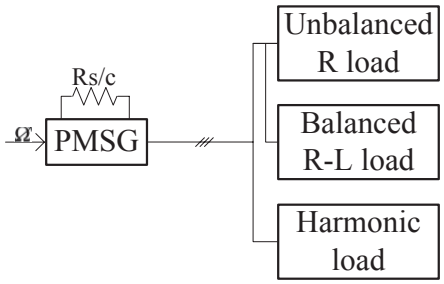

Figure 3. Simulation test bench scheme

B. Simulation Results

As shown in Figure 4(a), where a 16% inter-turn short-circuit is generated at t=0.5s on phase A, estimated parameters $n_{s/c}$ are impacted. Indeed, a modification of mean value and large oscillations at two times the electrical frequency appear as soon as the winding fault occurs. It is also noticeable that $n_{s/c1}$ is not the only estimated parameter sensitive to the short-circuit: $n_{s/c2}$ and $n_{s/c3}$ are also modified in a lower extent. However, the fault can clearly be located on phase A in this test. According to this test, the chosen indicator to detect inter-turn short-circuits expressed in (4) is based on the sliding average value of these parameters over one electrical half period.

$$\text{Fault\_indicator} = \sum_{i=1}^{3} \left\langle \left| \mathbf{n_{s/c}} \right|_i \right\rangle_{T/2} \quad (4)$$

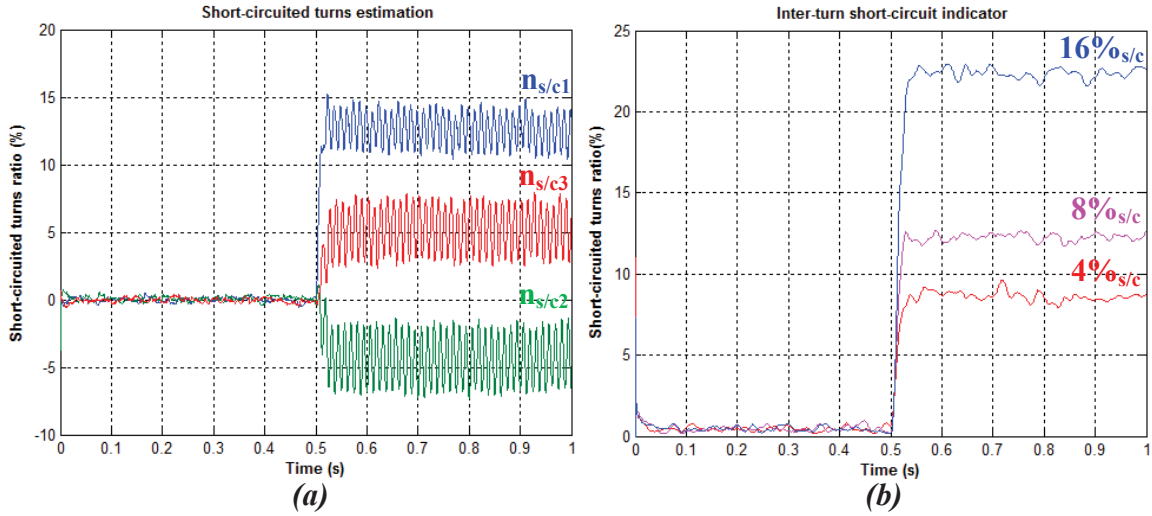

Figure 4. Simulation results. (a) Estimated parameters response to a 16% inter-turn short-circuit. (b) Fault indicator response to various inter-turn short-circuits

Figure 4(b) shows the evolution of this fault indicator in healthy case (for t < 0.5s) and in faulty case (for t > 0.5s) with several values of short-circuited turns on phase A. In healthy case, the fault indicator remains closed to 0, reflecting a safe PMSG. In faulty cases, the fault indicator increases with the number of short-circuited presented, which confirms that the fault detection is trickier for a few number of turns short-circuited. Moreover, time response of the chosen indicator remains quick (about 20 ms) in spite of the filtering characteristic of the sliding mean calculation. In the following section, the effectiveness of this fault indicator is evaluated against several operating points and several inter-turn short-circuit.

IV. Fault Indicator Performance Assessment

A. Robustness Assessment

In order to evaluate the robustness of the chosen fault indicator to the inter-turn short-circuit diagnosis, several simulation tests based on Figure 3 have been made such as frequency, power load, power factor, unbalanced load and harmonic load variation tests. The robustness is then characterized by the ability of the EKF algorithm to properly separate the healthy and the faulty cases whatever the operating conditions. To quantify this ability, healthy and faulty simulations are performed under the same operating conditions and the worst indicator's value is kept for each test (i.e. the highest indicator's value in healthy case and the lowest indicator's value in faulty case). The following spider charts (Figure 5) summarize the robustness of the chosen indicator against electrical network variation by comparing healthy and faulty operation with several short-circuited turns. It indicates that an inter-turn short-circuit fault can easily be segregated to a healthy PMSG whatever the operating conditions.

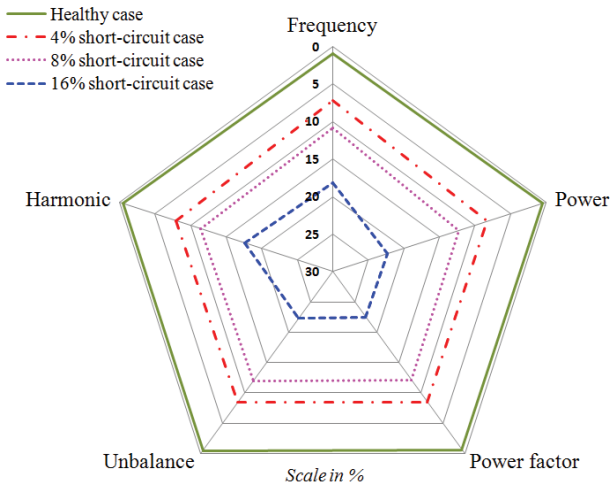

Figure 5. Robustness spider chart

B. Sensitivity Assessment

To evaluate the sensitivity of the chosen indicator, an appropriate detection threshold is firstly set to prevent false alarms in safe configuration whatever the operation conditions (for this indicator, the threshold is set to 2%). Secondly, the minimum fault current required to detect an inter-turn short-circuit according to the threshold is determined. Figure 6 summarizes this sensitivity test in which the short-circuit resistance $R_{s/c}$ is used to vary the inter-turn short-circuit severity. This test confirms that the fault detection is trickier and more critical for a few number of turns short-circuited. Indeed, in relation to the 15A rated current of the studied PMSG, a fault current of 48A is required to detect a 4% inter-turn short-circuit compared to a 15A fault current required to detect a 16% inter-turn short-circuit. However, stator windings of a PMSG can easily withstand three times the rated current during the detection time. Moreover, these results shows that an early detection when a resistive inter-turn short-circuit occurs is possible with this chosen indicator even for a few number of short-circuited turns.

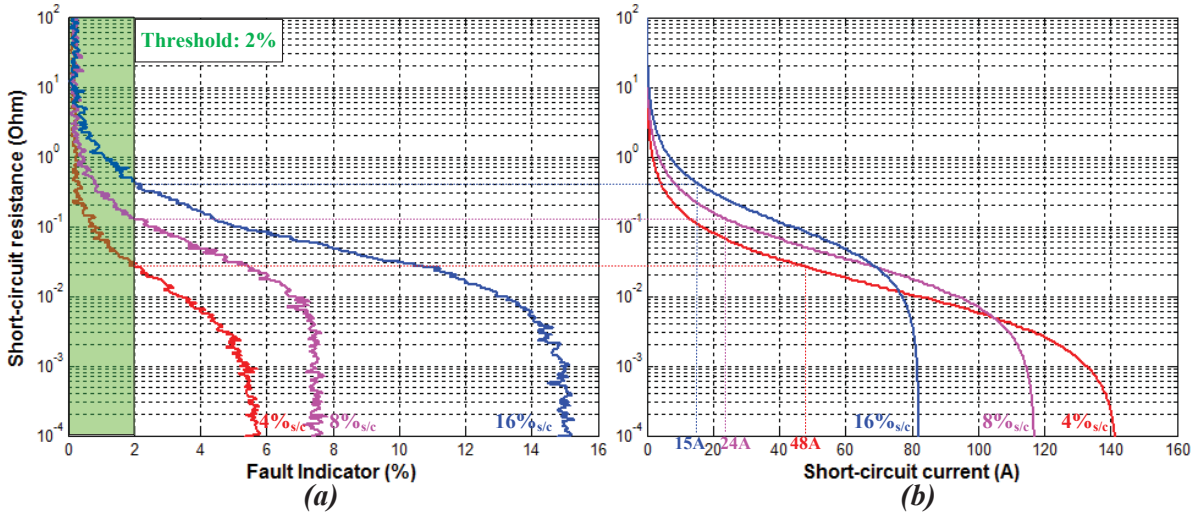

Figure 6. Sensitivity test. (a) Fault indicator vs short-circuit resistance. (b) Short-circuit current vs short-circuit resistance

V. Conclusions

This paper described a method for inter-turn short-circuit detection in stator windings based on a short-circuit turns estimation on a faulty PMSG model using an EKF algorithm. This fault diagnosis enables a fast and robust detection of inter-turn short-circuit whereas the operating conditions on a non ideal electrical network. The prospects of this work are to validate the simulation results on an experimental test bench.

References

[1] J.E. Hill, S. Mountain, "Control of a Variable Speed, Fault Tolerant Permanent Magnet Generator", *IEE International Conference on Power Electronics, Machines and Drives (PEMD 2002),* pp. 492-497, June 2002.

[2] D.M. Saban, C. Bailey, D. Gonzalez-Lopez and L. Luca, "Experimental evaluation of a high-speed permanent-magnet machine", *Proc. 55th IEEE PCIC*, pp.1 -9 2008.

[3] S. M. A. Cruz and A. J. M. Cardoso, "Multiple reference frames theory: A new method for the diagnosis of stator faults in three-phase induction motors", *IEEE Trans. Energy Convers.*, vol. 20, no. 3, pp.611 -619 2005.

[4] S. Bachir, S. Tnani, J.-C. Trigeassou and G. Champenois, "Diagnosis by parameter estimation of stator and rotor faults occurring in induction machines", *IEEE Trans. Ind. Electron.*, vol. 53, no. 3, pp.963 -973 2006.

[5] D. Diallo, M. E. H. Benbouzid, D. Hamad and X. Pierre, "Fault detection and diagnosis in an induction machine drive: A pattern recognition approach based on Concordia stator mean current vector", *IEEE Trans. Energy Convers.*, vol. 20, no. 3, pp.512 -519 2005.

[6] A. Ali Abdallah, J. Regnier, J. Faucher, "Simulation of Internal Faults in Permanent magnet Synchronous Machines", *6th International Conference on Power Electronics and Drive Systems*, Kuala Lumpur, Malaysia, 2005.